

Band-offset determination of the CdTe/(Cd,Mn)Te interface

T. Lebihen, E. Deleporte, and C. Delalande

Laboratoire de Physique de la Matière Condensée de l'École Normale Supérieure, 24 rue Lhomond, 75231 Paris Cedex 05, France

(Received 2 August 1996)

We report on photoluminescence excitation spectroscopy of CdTe/(Cd,Mn)Te separate confinement heterostructures. The Mn concentration and layers thicknesses are carefully chosen, so that transitions that are strongly dependent on the valence-band offset are observable. Comparison between theory and experiments gives a valence-band offset between CdTe and Cd_{1-x}Mn_xTe equal to 25% ± 7% of the total band-gap difference. [S0163-1829(97)06504-1]

I. INTRODUCTION

Among various II-VI systems, the growth by molecular-beam epitaxy of semimagnetic heterostructures, like CdTe/(Cd,Mn)Te, ZnSe/(Zn,Mn)Se or ZnSe/(Zn,Fe)Se, is increasingly well controlled.¹⁻⁵ The study of such heterostructures has opened a large area of new phenomena such as magnetic-field-induced type-I/type-II transition⁶ or spin superlattices,⁴ because of the large variation of the conduction- and valence-band edges as a function of an applied magnetic field. This large variation results from the exchange interaction between the carriers and the magnetic ions spins. Precise knowledge of the band alignment is important to understand the properties of these heterostructures. A great amount of work has been done, in particular, in CdTe/(Cd,Mn)Te, concerning the determination of the valence- and conduction-band offsets. But the relative valence-band offset q_v , defined as the percentage of the gap difference between the binary and ternary alloys lying in the valence band, is still a topic of controversy: see Table I where some q_v values are compiled.

Theoretical evaluations of q_v yield very different results

(see Table I). In fact, these calculations involve the surface charges distribution induced by dipolar interactions at the interfaces, and this distribution is very difficult to modelize. Experimental techniques like x-ray photoemission spectroscopy (XPS) or ultraviolet photoemission spectroscopy provide interesting information about the interfaces but give the value of q_v with poor accuracy. In a similar way, the q_v determinations involving a fit of the excitonic optical transitions energies in single quantum wells are not accurate. On the contrary, the q_v determinations that use a comparison between the experimental and theoretical magnetic dependence of the excitonic transitions are very precise, but the absolute value of q_v can be wrong. The problem arises from the control of the sharpness of the interfaces, which can modify the penetration of the electronic wave functions in the semimagnetic (Cd,Mn)Te barrier and therefore their magnetic dependence.²⁰ Moreover, a possible modification of the antiferromagnetic interaction between neighboring manganese ions in the interface vicinity could also alter every determination of q_v based on magneto-optical properties.²¹

TABLE I. Different values of q_v found in the literature. The structures studied in the reported references are CdTe/Cd_{1-x}Mn_xTe heterostructures, where x is the Mn concentration. The method used for the q_v determination is indicated.

Ref.	Structure	x	Method used for the q_v determination	q_v (%)
7	CdTe/MnTe interface	1	Calculation	28.2
8	CdTe/MnTe interface	1	Calculation	47
9 and 10	thin Cd _{1-x} Mn _x Te films grown on CdTe substrates	From 0 to 0.9	XPS	0
11	superlattices	0.24	Magneto-optical study	6.5
12	quantum wells	0.2	Magneto-optical study	10
13	multiple-quantum wells	1	Magneto-optical study	0-18
14	quantum wells	1	$E_1L_1 - E_1H_1$ difference	17
6	superlattices	0.07	Magnetic-field-induced type I-type II	15-20
15	multiple-quantum wells	0.12 and 0.27	$E_1L_1 - E_1H_1$ difference	30
16	multiple-quantum wells	0.05	Magneto-optical study	25-40
17	superlattices	0.066	Magneto-optical study	40
18	multiple-quantum wells	0.08	Magneto-optical study	40
19	multiple-quantum wells	0.07	Spin-flip Raman under a magnetic field	46

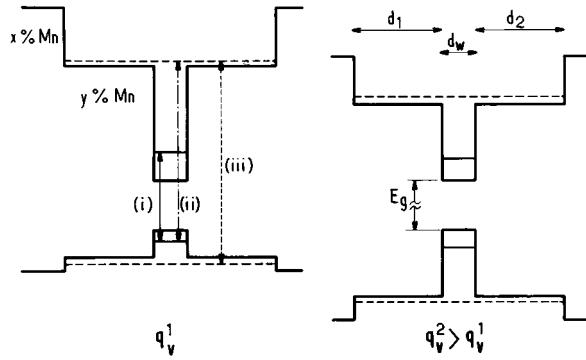


FIG. 1. Schematized representation of the QWSCH potential profile for two values of the relative valence-band offset q_v , showing the three kinds of optical transitions.

In this paper, we use a determination of q_v that is completely independent of magnetic properties. The basic idea is to find a heterostructure so that there are optical transitions strongly dependent on q_v . Quantum-well separate confinement heterostructures (QWSCH's) are such heterostructures. They have already been used in systems like GaAs/(Ga,Al)As (Ref. 22) and CdTe/(Cd,Zn)Te (Ref. 23) to determine the band offset. As recalled schematically in Fig. 1, a QWSCH consists of a CdTe well embedded in a larger Cd_{1-y}Mn_yTe well (called the intermediate barrier), and this structure is surrounded by a Cd_{1-x}Mn_xTe barrier of larger Mn concentration. Three kinds of optical transitions can be observed in a QWSCH depending on where the conduction and valence states are confined: (i) both of them are in the narrow CdTe well, (ii) one lies in the CdTe well and the other lies in the intermediate barrier (these kinds of transitions are called hybrid transitions), (iii) both of them are in the intermediate barrier. When q_v increases, the variations of the electron and hole confinements partially compensate each other for the (i) and (iii) transitions. On the contrary, the difference in energy spacing between adjacent levels of the CdTe well and of the intermediate barrier induces a strong dependence on the conduction and valence barrier heights for the energies of (ii) transitions. As a consequence, the hybrid transitions are well suited to determine q_v .

We report on photoluminescence and photoluminescence excitation spectroscopy experiments performed on two QWSCH's in which there are hybrid transitions having a nonzero oscillator strength. The experimental results are compared to the calculated ones. After the sample is carefully characterized, the hybrid transitions are identified: we find a relative valence-band offset: $q_v = 25\% \pm 7\%$. The influence of the interface quality on this result is discussed: we show that the existence of an interface mixing does not modify the value of q_v we have obtained.

II. EXPERIMENTS

The two studied samples *A* and *B* are quantum-well separate confinement heterostructures whose nominal parameters are reported in Table II. Sample *A* is grown on a very thick 3.6- μm Cd_{1-x}Mn_xTe buffer layer, deposited on a 270 Å CdTe layer, deposited on a Cd_{0.96}Zn_{0.04}Te substrate. On the buffer layer, a d_1 thick Cd_{1-y}Mn_yTe layer, then a d_w CdTe

TABLE II. Nominal values and measured values with their uncertainty of the concentrations and layer thicknesses for samples *A* and *B*.

Parameters	Nominal value	Measured value with its uncertainty
Sample <i>A</i>		
x (%)	30	25.7 ± 0.2
y (%)	20	18.5 ± 0.2
d_1 (monolayers)	25	
d_w (monolayers)	9	8 ± 1
d_2 (monolayers)	25	
Sample <i>B</i>		
x (%)	30	29 ± 0.2
y (%)	20	19.3 ± 0.2
d_1 (monolayers)	5	
d_w (monolayers)	22	25 ± 2
d_2 (monolayers)	0	

layer, and then a d_2 Cd_{1-y}Mn_yTe layer are successively grown. Sample *B* is grown on a 2000 Å-thick Cd_{1-x}Mn_xTe buffer layer, deposited on a Cd_{0.88}Zn_{0.12}Te substrate. On the buffer layer, a d_1 thick Cd_{1-y}Mn_yTe layer, then a d_w CdTe layer, and then a d_2 Cd_{1-y}Mn_yTe layer are successively grown. A 250-Å-thick Cd_{1-y}Mn_yTe layer is grown 500 Å after the QWSCH. On top of the two samples, there is a 500-Å-thick cladding layer.

Photoluminescence and excitation spectroscopy measurements are performed at low temperature ($T=2$ K) using standard cw laser excitation and lock-in techniques. Figure 2 shows the photoluminescence and excitation spectra of sample *A*. The excitation spectrum exhibits several peaks whose light- (lh) or heavy- (hh) hole nature has been determined by means of magnetoexcitation spectroscopy, performed up to 5.5 T with a superconducting magnet in the Faraday configuration. In such semimagnetic materials, heavy-hole transitions exhibit a larger Zeeman splitting than the light-hole transitions.²⁴ Note that the magnetic field is

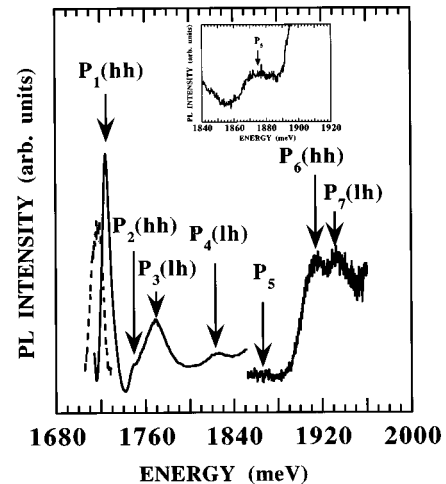


FIG. 2. Photoluminescence (dashed line) and photoluminescence excitation spectroscopy (solid line) of sample *A*. The inset is an enlargement of the P_5 line.

TABLE III. Minimum, maximum, and average values of the material parameters used in the calculation of the excitonic transition energies. The contribution of each material parameter to the uncertainty on q_v , named Δq_v , is evaluated.

Parameter	Notation	Minimum value	Maximum value	Average value	Δq_v (%)
Effective masses along the growth axis (in units of m_0 , the free-electron mass)	m_e	0,088 (Ref. 26)	0,11 (Ref. 27)	0,099	± 0.5
	m_{hh}	0,4 (Ref. 28)	0,66 (Ref. 29)	0,53	± 1
	m_{lh}	0,11 (Ref. 29)	0,159 (Ref. 30)	0,1345	± 0.5
Luttinger parameters	γ_1	3,9 (Refs. 30 and 29)	5,595 (Refs. 27 and 28)	4,7475	± 2
	γ_2	0,95 (Refs. 28 and 30)	1,894 (Refs. 27 and 29)	1,422	± 1.5
CdTe band-gap energy (meV)	E_g	1606 (Ref. 31)	1606,1 (Ref. 31)	1606.05	± 0
Cd $_{1-x}$ Mn $_x$ Te band-gap energy: $E'_g = E_g + \Delta E_g x$ (meV)	ΔE_g	1564 (Ref. 32)	1592 (Ref. 31)	1578	± 0.25
Ratio of the elastic constants	S_{11}/S_{12}	-2,424 (Ref. 33)	-2,57 (Ref. 34)	-2,497	± 0.5
Deformation potentials (eV)	a_c	2,151 (Refs. 35 and 36)	3,114 (Refs. 37 and 38)	2,6325	± 0
Cd $_{1-x}$ Mn $_x$ Te lattice parameter $a(x) = a_1 + a_2 x$ (Å)	a_v	-1,215 (Refs. 35 and 37)	-0,4 (Refs. 35 and 38)	-0,8075	± 0.25
	b_v	-1,22 (Ref. 34)	-1,06 (Ref. 39)	-1,195	± 0
	a_1	6,481 (Ref.40)	6,486 (Ref. 31)	6,4835	± 0
Dielectric constant	a_2	-0,138 (Ref. 41)	-0,152 (Ref. 42)	-0,145	± 0
	$\kappa(0)$	9,4 (Ref. 31)	10,6 (Ref. 31)	10	± 0.5

used here only to discriminate the heavy- and light-hole nature of the transitions and will not be involved in the determination of q_v . The nature of the P_5 line could not be evaluated: the intense neighboring P_6 line exhibits a huge Zeeman splitting and the P_5 line is hidden even for small magnetic fields.

In order to assign the peaks observed in the excitation spectrum, we compare their experimental energy positions with calculated excitonic transition energies. The variational calculation of the excitonic transition energies is reported in detail in Ref. 25. It takes into account the strain and excitonic effects. This calculation is valid for a type-I (electrons and holes localized in the same layer) and a type-II (electrons and holes localized in adjacent layers) structure. The values of the material parameters used in the calculation, effective masses, band gaps, dielectric constant, deformation potentials, elastic constants, and lattice parameters, are reported in Table III. As a great dispersion on the value of these parameters exists in the literature, we compile in Table III their minimum, maximum, and average values.

The two first experimental intense transitions P_1 (hh) and P_3 (lh) are naturally assigned to the fundamental E_1H_1 and E_1L_1 excitonic transitions, respectively. The levels E_1 , H_1 , and L_1 being well confined in the CdTe well potential, E_1H_1 and E_1L_1 are not sensitive to x , d_1 , d_2 , y . On the contrary, because the CdTe well is thin, E_1H_1 and E_1L_1 are very sensitive to d_w . The comparison between the experimental and theoretical energies provides $d_w = 8 \pm 1$ monolayers. The P_2 (hh) line, which lays 23 meV higher than E_1H_1 , and which appears to be rather a plateau than a peak, can be reasonably assigned to the $2s$ level or onset of the continuum of the E_1H_1 exciton.

Before assigning all the peaks and identifying the hybrid

transitions, the sample has to be carefully characterized and the real values of the sample parameters x , y , d_1 , d_2 have to be determined. The thickness of the intermediate barrier is large (190 Å) and the states confined in the Cd $_{1-y}$ Mn $_y$ Te layers, like the states confined in the CdTe layer, are not sensitive to d_1 and d_2 , so we will use the nominal values of d_1 and d_2 . The x concentration and the strain state of the heterostructure are determined by performing the excitation spectrum of the Cd $_{1-x}$ Mn $_x$ Te barrier photoluminescence. No heavy-hole–light-hole splitting of the fundamental exciton of the barrier can be resolved. This attests that the strain in the barrier is zero: the barrier layer is completely relaxed. The thickness $d_1 + d_w + d_2$ being inferior to the critical thickness [about 1000 Å (Ref. 3)], we reasonably assume an elastic accommodation of the Cd $_{1-y}$ Mn $_y$ Te and CdTe layers lattice parameters on the Cd $_{1-x}$ Mn $_x$ Te layer lattice parameter: we find that the heterostructure is compressed. The energy position of the fundamental exciton of the barrier allows the determination of x : taking the average energy gap parameter reported in Table III and a value of the exciton binding energy in Cd $_{1-x}$ Mn $_x$ Te: $E^{3D} = 11$ meV [the same value as in CdTe (Ref. 31)], we find $x = 25.7\% \pm 0.2\%$ (the uncertainty $\pm 0.2\%$ comes from the experimental error on the energy position). The value of x thus determined is reported in Table II. To determine y , we take the P_7 line, identified as the E_2L_2 transition, for which the electronic and hole levels lay in the Cd $_{1-y}$ Mn $_y$ Te layer. We deduce $y = 18.5\% \pm 0.2\%$ when taking the average set of material parameters.

Figure 3 shows the calculated excitonic transitions versus the valence-band offset, taking the average values of the material parameters and the afore-determined sample parameters reported in Table II: the (i) transitions are reported as solid lines, (iii) transitions as dashed lines, (ii) transitions as

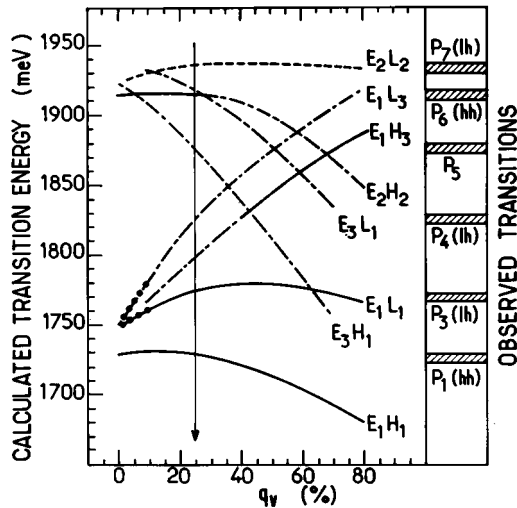


FIG. 3. Calculated excitonic transitions versus q_v and energy position of the experimental peaks for sample A. Solid lines are (i) transitions, dashed lines are (iii) transitions, dashed-dotted lines are hybrid transitions, and dotted lines are type-II transitions. The thickness of the lines representing the observed transitions is the uncertainty on the energy position of the experimental peaks.

dashed-dotted lines. Because of the strain, electrons and holes can be localized in adjacent layers (type-II structure) for small q_v : for example, the E_1L_1 and E_1L_3 transitions are type-II for $q_v < 10\%$; these type-II transitions are reported as dotted lines in Fig. 3. The existence of several hybrid transitions can be seen and their large dependence on q_v can be noted, confirming the validity of our q_v determination method. Note that the (i), (ii), or (iii) nature of the transitions depends on q_v : for example, E_2H_2 is a (iii) transition for $q_v < 35\%$ and thus is not sensitive to q_v ; it is a hybrid transition for $q_v > 35\%$ and thus is very sensitive to q_v .

From Fig. 3, it is possible to assign all the peaks observed in the excitation spectrum; the thickness of the lines representing the observed transitions is the experimental error on the energy position of the lines. The $P_3(\text{lh})$ and $P_6(\text{hh})$ peaks are assigned without any ambiguity to E_1L_1 and E_2H_2 , respectively. The E_1H_3 transition is not observed experimentally because it is hidden by the intense E_1L_1 peak. The P_5 and $P_4(\text{lh})$ lines turn out to correspond to the E_3H_1 and E_1L_3 hybrid transitions, respectively, E_1 and H_1 being confined in the CdTe well, L_3 and E_3 being delocalized over the $\text{Cd}_{1-y}\text{Mn}_y\text{Te}$ intermediate barrier. A good fit between the experimental data and calculated results using the set of average material parameters is found for $q_v = 25\%$.

The same study has been performed on sample B. The x concentration and the strain state have been determined from the excitation spectroscopy of the $\text{Cd}_{1-x}\text{Mn}_x\text{Te}$ barrier luminescence: $x = 29 \pm 0.2\%$. The $\text{Cd}_{1-x}\text{Mn}_x\text{Te}$ layers are relaxed and the QWSCH is compressed. The y concentration is deduced from the excitation spectroscopy of the wide 250-Å $\text{Cd}_{1-y}\text{Mn}_y\text{Te}$ well: the $\text{Cd}_{1-y}\text{Mn}_y\text{Te}$ well being large, the E_1H_1 transition of this well will not be sensitive to the well thickness but very sensitive to y , we obtain $y = 19.3\% \pm 0.2\%$. The d_w value comes from the identification of the E_1H_1 transition of the QWSCH as for the previous sample: $d_w = 25 \pm 2$ monolayers. As in the previous sample, the

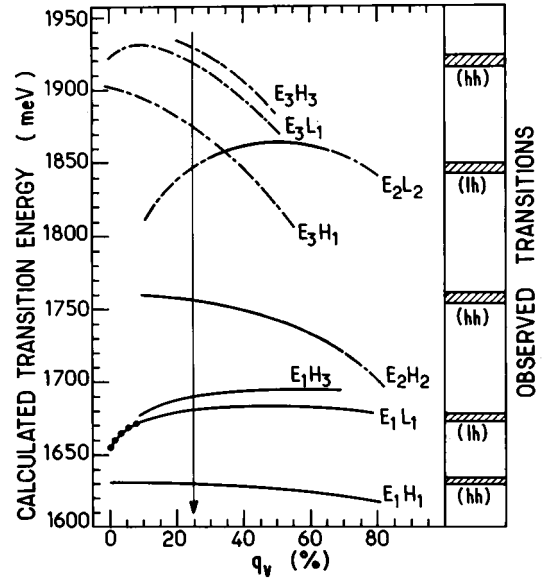


FIG. 4. Calculated excitonic transitions versus q_v , and energy position of the experimental peaks for sample B. Solid lines are (i) transitions, dashed-dotted lines are hybrid transitions, and dotted lines are type-II transitions. The thickness of the lines representing the observed transitions is the uncertainty on the energy position of the experimental peaks.

nominal values of d_1 and d_2 will be used. The comparison between the experimental and theoretical results is shown in Fig. 4 for sample B. The E_1H_3 transition is not seen experimentally because it is hidden by the intense E_1L_1 peak. E_3H_1 and E_3L_1 transitions are not expected to be seen experimentally because the oscillator strengths of these transitions are 100 times smaller than the neighboring transitions E_2L_2 and E_3H_3 . As for sample A, a good fit is obtained for $q_v = 25\%$, when taking the average set of material parameters.

This value of q_v has been determined using the set of the average material parameters in the calculation. The error on q_v mostly arises from the great dispersion existing on the values of the material parameters. So the comparison between theoretical and experimental results has to be performed for all the possible sets of material parameters: we evaluate $q_v = 25\% \pm 7\%$. The contribution of each material parameter to the uncertainty on q_v has been evaluated and reported in Table III. It can be seen that the largest contribution comes from the mass parameters. The strain parameters (S_{11}/S_{12} , a_c , a_v , b_v , a_1 , a_2) give small contributions because their only effect is to produce a global shift of all the excitonic transitions energies.

The magneto-optical properties of the heterostructure are not used to determine q_v in this paper. So we expect that our result is weakly dependent on the interface quality. Let us evaluate the influence of the interface mixing on our determination of q_v . Following the work of Gaj *et al.*,²⁰ it is possible to get quantitative information about the interface quality from the study of the Zeeman splitting of the fundamental exciton E_1H_1 . Figure 5 shows the E_1H_1 experimental Zeeman splitting (dots) obtained for sample A. The dashed line is the calculated E_1H_1 Zeeman splitting considering an abrupt interface without mixing and taking the average set of

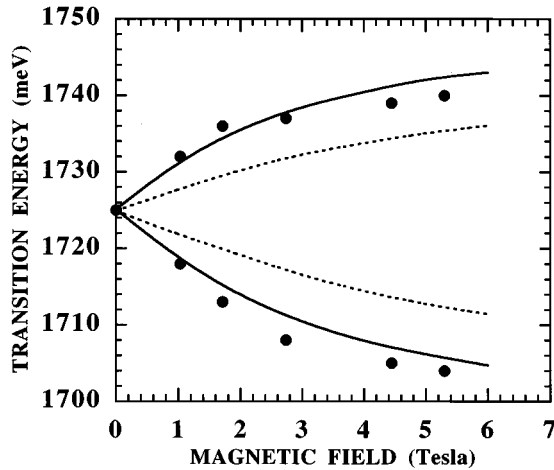


FIG. 5. Zeeman splitting of the E_1H_1 excitonic transition of sample A. Experimental values are reported as dots, the dashed line is the calculated Zeeman splitting taking the average set of material parameters, $q_v = 25\%$ and assuming abrupt interfaces. The solid line is the calculated Zeeman splitting taking $q_v = 25\%$ but assuming nonabrupt interfaces as explained in the text.

material parameters. It can be seen that the theoretical results do not fit the experimental results for the obtained value of $q_v = 25\%$. Gaj *et al.*²⁰ have shown that taking into account the interface mixing in the excitonic transition calculation allows us to reproduce the experimental results. We have calculated the excitonic transitions taking into account the existence of nonabrupt interfaces. Following Gaj *et al.*,²⁰ we have modeled the interface profile by an exponential function, in which a diffusion length L_d is defined. A good fit of the experimental Zeeman splitting is obtained for $L_d = 3 \text{ \AA}$ when taking $q_v = 25\%$, as can be seen in Fig. 5. This value is quite coherent with the diffusion lengths found by Gaj *et al.*²⁰ on samples grown in the same molecular-beam-epitaxy machine. Note that if we do not take into account the interface mixing in the calculations, we would have found a good fit between experimental and theoretical magnetic dependence of the excitonic transitions for $q_v = 5\%$: if the interface mixing is not taken into account, the q_v values obtained from magneto-optical experiments are underestimated.

We have checked that the variations of the transition energies versus the sample parameters like d_w , y , and versus the material parameters like effective masses, do not depend on the interface quality. So the energy differences between the excitonic transitions, calculated in the case of abrupt and nonabrupt interfaces, are the same whatever the set of parameters used in the calculation is. Only the absolute value of the excitonic transitions energies is altered. We find that, for a diffusion length $L_d = 3 \text{ meV}$, the absolute value of the excitonic transitions energies is modified by a value which is inferior to the experimental uncertainty (typically 3–4 meV). So the existence of the interface mixing does not alter our q_v determination.

III. CONCLUSION

In summary, we have determined the value of the relative valence-band offset in CdTe/(Cd,Mn)Te, $q_v = 25\% \pm 7\%$, by means of optical experiments on separate confinement heterostructures. These heterostructures allow the observation of optical transitions involving states localized in the CdTe or Cd_{1-y}Mn_yTe layers. Among these transitions, those involving a state in the CdTe layer and the other in the Cd_{1-y}Mn_yTe layer are very sensitive to the valence-band offset. Comparison between the observed transition energies and the calculated ones yields the value of q_v . The uncertainty on the q_v determination, due to the dispersion existing in the values of the material parameters used in the calculation, has been carefully evaluated. We point out that our method does not use the magneto-optical properties of CdTe/(Cd,Mn)Te heterostructures. So our q_v determination cannot be altered by the modifications of the magnetic properties due to the interface mixing. Moreover, we have explicitly checked that the existence of an interface mixing does not modify the obtained value of q_v .

ACKNOWLEDGMENTS

We would like to thank Guy Feuillet for the growth of the samples. The Laboratoire de Physique de la Matière Condensée is "Laboratoire associé au CNRS (URA 1437) et aux Universités Paris VI et Paris VII."

¹S. K. Chang, A. V. Nurmikko, J. W. Wu, L. A. Kolodziejski, and R. L. Gunshor, *Phys. Rev. B* **37**, 1191 (1988).

²A. Wasiela, Y. Merle d'Aubigné, J. E. Nicholls, D. E. Ashenford, and B. Lunn, *Solid State Commun.* **76**, 263 (1990).

³Le Si Dang, R. André, C. Bodin-Deshayes, J. Cibert, H. Okumura, G. Feuillet, and P. H. Jouneau, *Physica B* **185**, 551 (1993).

⁴X. Liu, A. Petrou, J. Warnock, B. T. Jonker, G. A. Prinz, and J. J. Krebs, *Phys. Rev. Lett.* **63**, 2280 (1989).

⁵E. Deleporte, T. Lebihen, B. Ohnesorge, Ph. Roussignol, C. Delalande, S. Guha, and H. MuneKata, *Phys. Rev. B* **50**, 4514 (1994).

⁶E. Deleporte, J. M. Berroir, G. Bastard, C. Delalande, J. M. Hong, and L. L. Chang, *Phys. Rev. B* **42**, 5891 (1990); G. Peter, E.

Deleporte, J. M. Berroir, C. Delalande, J. M. Hong, and L. L. Chang, *ibid.* **44**, 11 302 (1991).

⁷J. Tersoff, *J. Vac. Sci. Technol. B* **4**, 1066 (1986).

⁸M. Taniguchi, L. Ley, R. L. Johnson, J. Ghijsen, and M. Cardona, *Phys. Rev. B* **33**, 1206 (1986).

⁹G. Hollinger, in *Semiconductor Interfaces: Formation and Properties*, edited by G. Le Lay, J. Derrien, and N. Boccara, Springer Series in Physics Vol. 22 (Springer-Verlag, Berlin, 1987), p. 210.

¹⁰M. Pessa and O. Jylha, *Appl. Phys. Lett.* **45**, 646 (1984).

¹¹S. K. Chang and A. V. Nurmikko, *Phys. Rev. B* **37**, 1191 (1988).

¹²B. Kuhn-Heinrich, M. Popp, W. Ossau, A. Waag, and G. Landwehr, *Semicond. Sci. Technol.* **8**, 1239 (1993).

- ¹³T. J. Gregory, J. E. Nicholls, J. J. Davies, C. P. Hilton, W. E. Hagston, B. Lunn, and D. E. Ashenford, *Surf. Sci.* **228**, 359 (1990).
- ¹⁴N. Pelekanos, Q. Fu, J. Ding, W. Waleki, A. V. Nurmikko, S. M. Durbin, J. Han, M. Kobayashi, and R. L. Gunshor, *Phys. Rev. B* **41**, 9966 (1990).
- ¹⁵B. Kuhn-Heinrich, W. Ossau, T. Litz, A. Waag, and G. Landwehr, *J. Appl. Phys.* **75**, 8046 (1994).
- ¹⁶A. Wasiela, P. Peyla, Y. Merle d'Aubigné, J. E. Nicholls, D. E. Ashenford, and B. Lunn, *Semicond. Sci. Technol.* **7**, 571 (1992).
- ¹⁷A. Wasiela, Y. Merle d'Aubigné, J. E. Nicholls, D. E. Ashenford, and B. Lunn, *Solid State Commun.* **76**, 263 (1990).
- ¹⁸S. R. Jackson, J. E. Nicholls, W. E. Hagston, P. Harrison, T. Stirner, and J. H. C. Hogg, *Phys. Rev. B* **50**, 5392 (1994).
- ¹⁹M. P. Halsall, D. Wolverson, and J. J. Davies, *Solid State Commun.* **86**, 15 (1993).
- ²⁰J. A. Gaj, W. Grieshaber, C. Bodin-Deshayes, J. Cibert, G. Feuillet, Y. Merle d'Aubigné, and A. Wsiela, *Phys. Rev. B* **50**, 5512 (1994); P. Kossacki, Nguyen The Khoi, J. A. Gaj, G. Karczewski, T. Wojtowicz, J. Kossut, and K. V. Rao, *Solid State Commun.* **94**, 439 (1995).
- ²¹W. J. Ossau and B. Kuhn-Heinrich, *Physica B* **184**, 422 (1993).
- ²²M. H. Meynadier, C. Delalande, G. Bastard, M. Voos, F. Alexandre, and J. F. Liévin, *Phys. Rev. B* **31**, 5539 (1985).
- ²³E. Deleporte, J. M. Berroir, C. Delalande, N. Magnea, H. Mariette, J. Allegre, and J. Calatayud, *Phys. Rev. B* **45**, 6305 (1992).
- ²⁴A. Twardowski, T. Dietl, and N. Demianiuk, *Solid State Commun.* **48**, 845 (1983).
- ²⁵G. Peter, E. Deleporte, G. Bastard, J. M. Berroir, C. Delalande, B. Gil, J. M. Hong, and L. L. Chang, *J. Lumin.* **52**, 147 (1992).
- ²⁶Le Si Dang, G. Neu, and R. Romestain, *Solid State Commun.* **44**, 1187 (1982).
- ²⁷D. T. F. Marple, *Phys. Rev.* **129**, 2466 (1963).
- ²⁸B. Segall, *Phys. Rev.* **150**, 734 (1966).
- ²⁹P. Lawaertz, *Phys. Rev. B* **4**, 3460 (1971).
- ³⁰Ch. Neumann, A. Nöthe, and N. O. Lipari, *Phys. Rev. B* **37**, 922 (1988).
- ³¹*Numerical Data and Functional Relationship in Science and Technology*, edited by K. H. Hellwege, Landolt-Börnstein, New Series, Group III, Vol. 17, Pt. a (Springer-Verlag, Berlin, 1982).
- ³²D. Heiman, P. Becla, R. Kershaw, D. Ridgley, K. Dwight, A. Wold, and R. R. Galazka, *Phys. Rev. B* **34**, 3961 (1986).
- ³³D. Berlincourt, H. Jaffe, and L. R. Shiozawa, *Phys. Rev.* **129**, 1009 (1963).
- ³⁴D. J. Olego, J. Petruzello, S. K. Ghandi, N. R. Taskar, and I. B. Bhat, *Appl. Phys. Lett.* **51**, 127 (1987).
- ³⁵D. J. Dunstan, B. Gil, C. Priester, and K. P. Homewood, *Semicond. Sci. Technol.* **4**, 241 (1989); C. Priester, G. Allan, and M. Lannoo, *Phys. Rev. B* **38**, 13 451 (1988).
- ³⁶B. Gil and D. J. Dunstan, *Semicond. Sci. Technol.* **6**, 428 (1991).
- ³⁷M. Zigone, H. Roux-Buisson, H. Tuffigo, N. Magnea, and H. Mariette, *Semicond. Sci. Technol.* **6**, 454 (1991).
- ³⁸C. Van de Walle, *Phys. Rev. B* **39**, 1871 (1989).
- ³⁹H. Mathieu, J. Allègre, A. Chatt, P. Lefèvre, and J. P. Faurie, *Phys. Rev. B* **38**, 7740 (1988).
- ⁴⁰J. K. Furdyna and J. Kossut, in *Semiconductors and Semimetals: Diluted Magnetic Semiconductors*, edited by R. K. Willardson and A. C. Beer (Academic, New York, 1988), Vol. 25.
- ⁴¹J. R. Buschert, F. C. Peiris, N. Samarth, H. Luo, and J. K. Furdyna, *Phys. Rev. B* **49**, 4619 (1994).
- ⁴²S. M. Durbin, J. Han, Sungki O, M. Kobayashi, D. R. Menke, R. L. Gunshor, Q. Fu, N. Pelekanos, A. V. Nurmikko, D. Li, J. Gonsalves, and N. Otsuka, *Appl. Phys. Lett.* **55**, 2087 (1989).